SCRF-DFT and NMR Comparison of Tetracycline and 5a,6-Anhydrotetracycline in Solution

Olaf G. Othersen,[†] Reiner Waibel,[‡] Harald Lanig,[†,‡] Peter Gmeiner,[‡] and Timothy Clark*[,†]

Computer-Chemie-Centrum, Friedrich-Alexander-Universität Erlangen-Nürnberg, Nägelsbachstrasse 25, 91052 Erlangen, Germany, and Institut für Pharmazie und Lebensmittelchemie, Friederich-Alexander-Universität Erlangen-Nürnberg, Schuhstrasse 19, D-91052 Erlangen, Germany

Received: July 14, 2006; In Final Form: September 16, 2006

A combination of structures, energies, and spectral data calculated using density functional theory (DFT) with experimental NMR data has been used to assign conformational equilibria for tetracycline and 5a,6-anhydrotetracycline in water at pH 1, 7, and 10 and in chloroform (5a,6-anhydrotetracycline) and methanol (tetracycline). The results suggest that tetracycline always prefers the extended conformation but that 5a,6-anhydrotetracycline exists in water as a mixture of the two conformers and in chloroform exclusively in the twisted conformation. The conformational equilibria are also shown to be pH dependent.

Introduction

The tetracycline class of antibiotics[1] has achieved importance beyond their therapeutic use as broad-spectrum antibiotics because many tetracyclines are inducers of the tetracycline repressor protein (TetR), which has been used as an experimental switch to regulate gene expression.[2] Improving this functionality to be able to switch several genes with different inducers would be an invaluable experimental tool. However, to achieve this goal, it is necessary to understand the induction process of the TetR protein,[3] for which knowledge of the exact structures (conformations and tautomeric forms) of important tetracyclines in solution is essential. Tetracycline (Tc, **1**) and 5a,6-anhydrotetracycline (ATc, **2**) are possibly the most important representatives of the tetracyclines in this respect, as they not only interact differently with the TetR (ATc is a stronger inducer and can induce in the absence of magnesium ions[4]) but also are closely related structurally.

We have paid special attention to the protonation patterns in the O_{11} and O_{12} region, as the differences between **1** and **2**, apart from the obvious dehydration, the aromaticity of ring C, and the conformations of ring A,[5] are focused in this region. We have combined these theoretical studies with NMR measurements of the conformations of tetracyclines in solution. Comparing the theoretical and experimentally determined $J_{HH'}$ spin−spin coupling constants allows us to determine conformational equilibria. Earlier NMR[6] and circular dichroism[7] studies have suggested that two major conformations named "twisted" and "extended" exist in solution. These conformations differ in the relative positions of the carbon atoms C_1-C_{12a}, which we will designate as scaffold. The two major conformations will therefore be designated as "scaffold conformations" in the following, to distinguish them from conformations resulting from, for example, rotations of the amine or amide group.

We have focused primarily on the electrically neutral forms but have also used the results for the neutral forms as a basis for constructing conformations for differently charged structures.

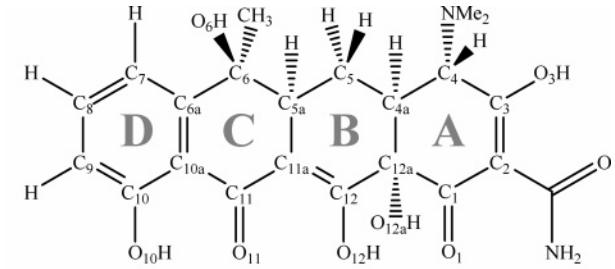

1

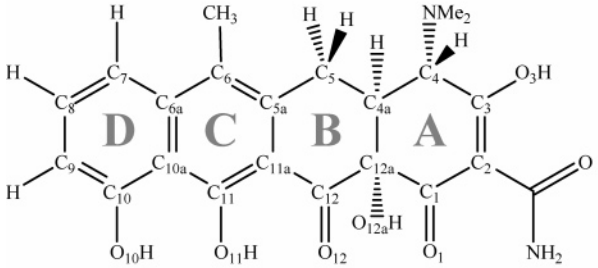

2

In the following we will describe the neutral forms as either nonionized or zwitterionic, reserving the term neutral to describe the total charge. We[8,9] and others[10] have previously reported density functional theory (DFT) and ab initio results for Tc[8] and ATc[9,10] but have now focused on a combined experimental/theoretical approach that allows us to provide quantitative estimates of the conformational equilibria for the first time. An additional motivation for revisiting these two systems was provided by improvements to the polarized-continuum model (PCM)[11] for solvent simulation between Gaussian 98[12] and Gaussian 03.[13] These improvements not only made it possible to consider all structures with the same variation of the PCM technique, which was not possible with Gaussian 98, but also resulted in small shifts in the calculated solvation energies, which made it necessary to recalculate the structures reported previously.

We now report a comprehensive DFT, ab initio, and NMR study to determine the relative importance of different tautomers

* To whom correspondence should be addressed. E-mail: clark@chemie.uni-erlangen.de.
[†] Computer-Chemie-Centrum.
[‡] Institut für Pharmazie und Lebensmittelchemie.

10.1021/jp064457s CCC: $33.50
Published on Web 11/14/2006

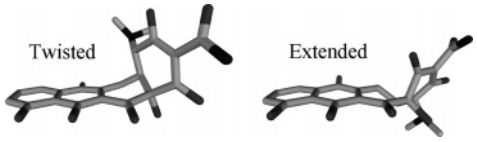

and conformations with special emphasis on the differences between the neutral forms of Tc and ATc and the energetic influence of different tautomers and hydrogen bonds. We also report combined experimental/theoretical determinations of the conformational equilibria of tetracyclines in solution.

Computational Methods

Structurally related tautomers for the $O_{11}-O_{12}$ region were generated starting from the structures optimized previously,[8,9] in which either O_{11} or O_{12} was protonated. These structures were adapted by rotating around the $-O_{11}-H$ or $-O_{12}-H$ groups and/or by transferring a proton between O_{11} and O_{12} to obtain a series of starting structures with $O_{12}H-O_{11}$ and $O_{11}H-O_{12}$ hydrogen bonds. Additional structures designed to help examine the proton tautomers of ring A were created from the nonionized minima of each conformation for **1** and **2** with either O_{11} or O_{12} being protonated. Three new input geometries were derived from each of these minima by shifting the O_3 proton to the O_{amide}, rotating the amide group by 180° around the C_2-C_{amide}, and shifting the O_{amide} proton to O_1.

The starting geometries were fully optimized in vacuo with Gaussian 03[13] using the Becke three-parameter hybrid functional[14] in conjunction with the Lee−Yang−Parr correlation functional[15] (B3LYP) and the 6-31G(d) basis set.[16] The structures obtained were confirmed as local minima by calculating their normal vibrations within the harmonic approximation. Single-point calculations on the optimized geometries using the self-consistent reaction field (SCRF) technique in simulated water or chloroform continua were used to account for solvent effects. The SCRF calculations used the standard polarizable continuum model with a cavity generated using the united-atom topological model (UAHF).[17] Single-point calculations with the same basis set were also performed with a second-order Møller−Plesset (MP2)[18] correction for electron correlation. Corrected MP2 relative energies (E_c) were calculated starting from the MP2/6-31G(d) energies (E_{MP2}) of the B3LYP/6-31G(d) optimized structures (E_{B3LYP}) and incorporating the B3LYP/6-31G(d) zero-point vibrational energy correction (E_{Freq}) and the UAHF−PCM B3LYP/6-31G(d) solvation energy correction[8,9] (E_{PCM}):

$$E_c = E_{MP2} + (E_{Freq} - E_{B3LYP}) + (E_{PCM} - E_{B3LYP}) \quad (1)$$

As discussed above, the SCRF calculations for the structures of Tc and ATc reported previously[8,9] were repeated with Gaussian 03 and the corrected MP2 relative energies E_c were calculated anew. In contrast to our earlier work with Gaussian 98,[12] no SCRF calculation failed; thus, the solvation energies could be treated consistently throughout.

To identify isomers with the same scaffold geometry but with differing protonation or hydrogen-bond patterns, the root−mean−square deviation (RMSD) between structures was calculated for the heavy atoms of every species with all others using the program Quatfit.[19] The C_6 atom and its substituents were omitted in the RMSD calculations for the RMSD between the Tc and ATc structures, as C_6 is hybridized differently. The tautomeric forms for the structure pairs with heavy-atom RMSDs below 0.25 Å were considered to have the same conformation. Their energies were compared directly to judge the effects of specific tautomeric shifts or rearrangements of hydrogen bond patterns on the stability. Energy changes for the same proton shift or conformational change within one species were combined, and the mean and standard deviation of the energy and RMSD differences were calculated to gain a more general set of principles governing the stability of different Tc and ATc structures.

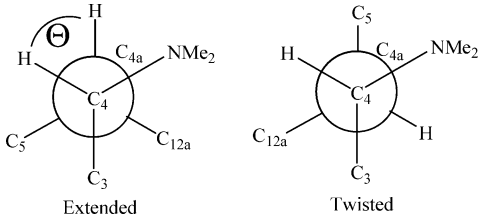

Figure 1. Newman projection along the C_4-C_{4a} bond in the extended and twisted conformations of tetracyclines.

Hydrogen bonds were defined by the distance between the hydrogen and the acceptor atom (<3 Å) and by the dihedral angle between the acceptor, the hydrogen, the donor, and the heavy atom bound to the donor. C_4 was used as the last atom defining the dihedral angle for the donor hydrogen of the amine group. Deviations from a planarity of less than 10° indicated hydrogen bonding. Bifurcated hydrogen bonding was examined by calculating the dihedral angle of an imaginary acceptor located at the geometric median of the real acceptors. If the dihedral deviation of the virtual acceptor from zero was less than 10°, hydrogen bonds to both acceptors were specified and, otherwise, a single hydrogen bond with the acceptor was specified with the smaller dihedral angle.

The chemical shifts and spin−spin coupling constants of the optimized structures were calculated in vacuo at the B3LYP/6-31G(d) level using the gauge-independent atomic orbital (GIAO) method.[20] To test whether the calculated spin−spin coupling constants depend on the solvent and charge, the extended and twisted minima for Tc and ATc in the nonionized and zwitterionic forms were used to calculate the spin−spin coupling constants in water and chloroform and to generate charged structures by adding or removing hydrogen atoms. Singly positively charged molecules were generated by adding a proton to the amine group for the nonionized forms and to O_3 for the zwitterionic forms. For the singly negatively charged structures, either the N_{amide}, the O_3, the O_{11}, or the O_{12} proton was removed. For the doubly negatively charged structures, all protons at these atoms were removed. The DFT calculation sequence defined above was also used for the charged structures, and the spin−spin coupling constants were calculated from the optimized structures.

The coupling constants were first directly compared to the experimental NMR measurements. To do this, the mean error between the complete set of experimentally observed coupling constants and the calculated coupling constants was determined for each structure. The scaffold conformations of the structures with the lowest mean errors (that is, those for which the calculations fit best to the experimental data) are given in the tables.

In a second step, the means and standard deviations of the vicinal spin−spin coupling constants between the protons of C_4 and C_{4a} ($^3J_{HH}(HC_4-HC_{4a})$) were used to calculate the equilibria for the different scaffold conformations. This coupling constant describes the conformation because it can be related to the dihedral angle Θ, which is different for the twisted and extended scaffold conformations (Figure 1), via the Karplus equation.[21]

TABLE 1: Calculated Relative Energies (kcal mol^{-1}) for Neutral Tetracycline Conformations and Tautomers[a]

			protonation state, acceptor							relative energy			
species	ref[8]	conf	O_{12a}	O_1	O_3	O_{11}	O_{12}	N_{amine}	O_{amide}	0 K	298 K	PCM (H_2O), 298 K	E_c (H_2O)
1_N1	**N1**	**E**	N_{amine}		O_{amide}		11			2.8	3.0	0.5	0.0
1_N2		**E**	N_{amine}				11		3	2.4	2.8	0.0	0.2
1_N3		**E**	N_{amine}	O_{amide}			11			2.7	2.9	0.6	0.3
1_N4		**E**	N_{amine}		O_{amide}	12				7.1	6.5	3.0	1.7
1_N5		**E**	N_{amine}			12			3	6.8	6.1	2.6	1.8
1_N6		**E**	N_{amine}			12			1	6.7	6.1	2.7	2.1
1_N7	**N2**	**E**	N_{amine}		O_{amide}		12a			9.4	9.2	4.9	2.4
1_N8		**E**	N_{amine}	O_{amide}		12				6.9	6.5	3.9	2.9
1_N9	**N3**	**T**	1		O_{amide}		11			0.0	0.0	2.8	3.3
1_N10		**T**	1				11		3	0.5	0.1	2.2	3.4
1_N11		**T**	1		O_{amide}	12				3.3	2.2	4.1	3.9
1_N12		**T**	1			12			3	3.6	2.7	4.0	4.4
1_N13	**N4**	**E**	12		O_{amide}		11			4.3	3.3	2.5	4.4
1_N14		**T**	1				11		1	1.6	1.6	3.6	4.6
1_N15		**E**	12		O_{amide}		11			4.3	3.4	2.8	4.7
1_Z1	**Z1**	**E**	1; 12				11	12a		23.2	24.5	9.5	3.8
1_Z2	**Z4**	**E**	12				11	3		27.0	26.3	8.6	5.5
1_Z3	**Z12**	**E**	1;12			12		12a		25.7	26.4	12.2	5.8
1_Z4	**Z6**	**E**	12					12a	3	28.2	28.5	10.1	6.6
1_Z5	**Z7**	**T**	1				11	6		23.5	25.5	11.4	7.0
1_Z6	**Z5**	**E**	1;12				1	12a		29.2	29.7	14.1	7.1
1_Z7	**Z9**	**T**	1				11	3		20.0	20.6	9.6	7.2
1_Z8	**Z3**	**E**	12		O_{amide}			12a		30.3	29.9	11.8	7.2
1_Z9		**E**	12			12		3		30.2	29.2	11.5	8.0
1_Z10	**Z8**	**E**	12	O_{amide}				12a		27.9	27.9	10.8	8.1
1_Z11	**Z15**	**T**	1			12		6		27.4	28.8	14.3	8.6
1_Z12	**Z14**	**T**	1			12		3		23.2	23.3	12.2	8.8

[a] Species are denoted by the molecule (**1**, tetracycline), the charge distribution (**N**, nonionized; **Z**, zwitterionic), and the ranking of the corrected MP2 relative energies (E_c) in water. The reference column gives the designation used for the structure in ref 8. In the conformation column, **E** indicates the conformation usually known as extended and **T** indicates twisted.[6,7] The protonation state columns indicate protonation if an entry is present. The entries in the columns then indicate the appropriate hydrogen bond acceptor. A blank entry indicates that the atom given in the column heading is not protonated. N_{amine} and O_{amide} indicate that the acceptor is either the Me_2N nitrogen or the amide oxygen, respectively. The MP2-corrected relative energies were calculated as described in the Computational Methods section.

The different dihedral angles Θ of the twisted and extended scaffold conformations (Figure 1) and their calculated values for $^3J_{HH}(HC_4-HC_{4a})$ made it possible to generate spin−spin coupling parameters for the extended (cp_E) and the twisted (cp_T) scaffold conformations by averaging their $^3J_{HH}(HC_4-HC_{4a})$ values.

Assuming that we can describe the equilibrium using only these two conformations and that the equilibrium is fast on the NMR time scale, we should observe averaged values for the different spin−spin coupling constants.[22] We can, therefore, calculate the fractions of the extended (P_E) and twisted (P_T) conformations in solution by measuring $^3J_{HH}(HC_4-HC_{4a})$ and assuming the calculated values for the "pure" extended and twisted conformations. The results can then be used to estimate an experimental free energy difference between the conformations by assuming a Boltzmann distribution.

Experimental Methods

The ^{1}H NMR spectra were measured at 600 MHz on a Bruker Avance spectrometer equipped with an inverse probe with a z-gradient coil using standard pulse programs. For water suppression, the sequence using presaturation composite pulses and spoil gradient was used.[23] $CDCl_3$, CD_3OD, and phosphate buffer in H_2O-D_2O (9:1) were used as the solvents, and tetramethylsilane and sodium-3-trimethylsilyl-2,2,3,3-d4-propionate were used as the internal standards. Due to the limited solubility of both Tc and ATc, the measurements in water at pH 7 were performed at 330 K.

Coupling constants were extracted from the ^{1}H NMR spectra received after zero filling from 32K to 128K data points and subsequent suitable Lorentz−Gauss transformation prior to Fourier transformation.

Results

Conformations. After eliminating identical structures, the calculations resulted in 21 (**1_N1**−**1_N21**) and 36 (**2_N1**−**2_N36**) nonionized conformations and 21 (**1_Z1**−**1_Z21**) and 38 (**2_Z1**−**2_Z38**) zwitterionic conformations for Tc and ATc, respectively. Tables 1 and 2 show the tautomeric forms, hydrogen bonds, and calculated relative energies for the minima obtained. Only the local minima within 5 kcal mol^{-1} of the corresponding absolute minimum (**1_N1**, **1_Z1**, **2_N1**, or **2_Z1**) are considered. The Microsoft Excel file provided as part of the Supporting Information lists the energies, tautomeric forms, and hydrogen bond data of all 116 structures.

All species adopt either the extended (**E**) or the twisted (**T**) conformation.[6,7] Compared to **T**, conformation **E** is favored in solution for Tc (**1**) by 3.3 kcal mol^{-1} for the nonionized form and 3.2 kcal mol^{-1} for the zwitterionic form, whereas for ATc (**2**) conformation **T** is 0.2 kcal mol^{-1} more stable for the nonionized form and 0.6 kcal mol^{-1} more stable for the zwitterionic form. The nonionized form is favored by 3.8 kcal mol^{-1} for **1** and 3.6 kcal mol^{-1} for **2**. This suggests that the same systematic error found earlier,[8,9] which disfavors the zwitterions by ∼3.5−4 kcal mol^{-1}, also applies to our current calculations. This error results partly from the tendency of the DFT and, to a lesser extent, MP2 calculations to underestimate the stability of the charge-separated species relative to their unionized counterparts. A second contributing factor is probably that the preferential solvation of the zwitterionic forms (and,

TABLE 2: Calculated Relative Energies (kcal mol^{-1}) for Neutral 5a,6-Anhydrotetracycline Conformations and Tautomers[a]

			protonation state, acceptor							relative energy			
species	ref[9]	conf	O_{12a}	O_1	O_3	O_{11}	O_{12}	N_{amine}(N)	O_{amide}(A)	0 K	298 K	PCM (H_2O), 298 K	E_c (H_2O)
2_N1		**T**	1		O_{amide}	12				0.0	0.3	0.2	0.0
2_N2		**T**	1			12			3	0.0	0.0	0.0	0.2
2_N3		**T**	1		O_{amide}	12				0.0	0.3	0.4	0.2
2_N4		**E**	N_{amine}		O_{amide}	12				6.6	6.9	1.8	0.2
2_N5		**E**	N_{amine}			12			3	6.1	6.6	1.4	0.4
2_N6		**E**	N_{amine}			12			1	6.1	6.5	1.5	0.7
2_N7		**E**	N_{amine}	O_{amide}		12				6.3	6.7	2.5	1.2
2_N8		**T**	1			12			1	0.8	1.2	1.3	1.3
2_N9		**T**	1	O_{amide}		12				3.0	2.8	2.5	2.3
2_N10		**T**	1		O_{amide}	12				4.3	3.8	2.9	3.0
2_N11		**T**	H		O_{amide}	12				9.4	8.9	5.0	4.2
2_N12	**N1**	**T**	1		O_{amide}		11			1.6	2.0	2.3	4.3
2_N13		**T**	1				11		3	1.7	2.1	1.9	4.3
2_N14		**E**	N_{amine}		O_{amide}		11			7.3	7.9	3.2	4.5
2_N15		**E**	12		O_{amide}	12				5.7	5.6	3.4	4.5
2_N16		**E**	N_{amine}				11		3	6.8	7.4	2.8	4.7
2_Z1	**Z1**	**T**	1			12		3		21.5	21.4	7.7	3.6
2_Z2	**Z3**	**E**	12			12		12a		24.9	26.4	10.9	4.2
2_Z3		**E**	12			12		12a		26.9	27.9	10.6	5.2
2_Z4	**Z4**	**E**	12			12		3		25.0	25.3	9.5	6.7
2_Z5	**Z7**	**T**	1			12		U		30.0	31.7	12.8	7.3
2_Z6	**Z2**	**T**	1				11	3		22.4	23.0	10.0	8.1
2_Z7	**Z13**	**E**	12					12a	3	32.6	33.8	9.9	8.2
2_Z8	**Z11**	**E**	12					12a	1	32.1	33.0	9.6	8.3

[a] Species are denominated by the molecule (**2**, 5a,6-anhydrotetracycline), the charge distribution (**N**, nonionized; **Z**, zwitterionic), and the ranking of the corrected MP2 relative energies (E_c) in water. The reference column gives the designation used for the structure in ref 9. In the conformation column, **E** indicates the conformation usually known as extended and **T** indicates twisted.[6,7] The protonation state columns indicate protonation if an entry is present. The entries in the columns then indicate the appropriate hydrogen bond acceptor. A blank entry indicates that the atom given in the column heading is not protonated, and H indicates protonation without a specific hydrogen-bonding partner. N_{amine} and O_{amide} indicate that the acceptor is either the Me_2N nitrogen or the amide oxygen, respectively. U denotes nonspecific hydrogen bonding. The MP2-corrected relative energies were calculated as described in the Computational Methods section.

most likely, specifically of the anionic centers) is slightly underestimated by the PCM solvation model. Experimentally, the zwitterionic form is found to predominate in solution,[6,7] from which we deduce the approximate magnitude of this systematic error.[8,9]

Hydrogen-Bonding Patterns. The hydrogen-bonding patterns found for the different structures were analyzed in detail, and the results are summarized in Table 3. The RMSDs between the heavy-atom scaffolds and the energy differences were calculated as outlined in the Computational Methods section.

Tables 1 and 2 show that almost all tautomers of **1** and **2** in the twisted conformation, **T**, contain an $O_{12a}H-O_1$ hydrogen bond. The only exception is **2_N11**, which is destabilized by 4.0 kcal mol^{-1} relative to the corresponding structure **2_N3** with the $O_{12a}H-O_1$ hydrogen bond, as shown in Table 3. The preferred hydrogen bond acceptor for $O_{12a}H$ in the extended conformation, **E**, is N_{amine} for the nonionized forms. For the zwitterionic forms, O_{12} always participates in the $O_{12a}H$ hydrogen bond, but less stable, bifurcated hydrogen bonding to O_1 and O_{12} as acceptors is also observed. Pure $O_{12a}H-O_1$ hydrogen bonding only occurs in high-energy structures.

The O_3 hydrogen atom prefers the O_{amide} as the acceptor with the exceptions of two high-energy structures, in which the amide group is rotated to enable O_3-N_{amine} hydrogen bonding. This alternative is 4.2 ± 1.5 kcal mol^{-1} less stable. $O_{11}H$ and $O_{12}H$ give $O_{11}H-O_{12}$ and $O_{12}H-O_{11}$ hydrogen bonds, respectively. Formation of the alternative $O_{12}H-O_1$ bond results in an energy loss of 7.8 ± 3.0 kcal mol^{-1} for **2**. The protonated amine acts as a hydrogen bond donor for O_{12a}, O_3, and O_6, but bifurcated H-bonding is also found for **2** in some cases. O_{12a} is the preferred acceptor for the extended conformation, **E**, whereas O_6 is energetically more stable in the same protonation pattern for the twisted conformation, **T**. However, the RMSD between the O_6 and O_3 hydrogen-bonded geometries is large, so the two scaffold structures do not correspond exactly. Structural comparison (Table 3) reveals the strength of the $N_{amine}H-O_3$ bond, which is 5.6 ± 0.4 kcal mol^{-1} more stable than a bifurcated hydrogen bond.

Tautomers. Tc (**1**) favors the protonation of O_{12} over O_{11} by 1.7 ± 0.6 kcal mol^{-1}, as shown in Table 3. In contrast, ATc (**2**) clearly prefers $O_{11}H$ over $O_{12}H$ (by 4.5 ± 1.3 kcal mol^{-1}). Ring A is very sensitive to proton shifts (Figure 2) in both conformations (**1_N1**−**1_N3**, **1_N9**, **1_N10**, **2_N1**, **2_N2**, **2_N4**, **2_N5**, **2_N7**).

The first protonation in the zwitteranionic forms always occurs at N_{amine}. The lowest-energy zwitterionic structures are deprotonated at O_3, while in some unfavorable cases deprotonation of the $O_{11}-O_{12}$ region is found (**1_Z8**). A second type of zwitterionic tautomer in which O_1 (**1_Z10**) or O_{amide} (**1_Z4**, **2Z_7**) is protonated by a formal hydrogen transfer from O_{11} or O_{12} is also observed.

Some pairs of structures with low scaffold RMSDs between the zwitterionic and the nonionized structures were found for **2**. Eight pairs prefer the nonionized form by 1.8 ± 1.5 kcal mol^{-1}, and three pairs prefer the zwitterionic form by 2.3 ± 0.2 kcal mol^{-1}. The RMSD (0.06 ± 0.00 Å) found for these three pairs is much smaller than the 0.18 ± 0.06 Å found for the eight pairs that preferred the nonionized form.

Structural Relationships between Tc and ATc. The calculated RMSDs (Table 4) show that the lowest energy structures of **1** and **2** have very similar scaffold conformations. We find structures that correspond closely for the two compounds in

TABLE 3: Mean Energy Differences and Their Standard Deviations for Related Conformers and Tautomers[a]

tautomeric change	no.	conf	Δ(RMSD) [Å]	Δ(energy) [kcal mol^{-1}]
		Tc (**1**)		
$O_3(A) \rightarrow O_{amide}(3)$	8	**E**, **T**	0.07 ± 0.02	0.2 ± 0.1
$O_{12}(11) \rightarrow O_{11}(12)$	16	**E**, **T**	0.10 ± 0.06	1.7 ± 0.6
$O_{12}(11) \rightarrow N_{amine}(12a)$; $H{:}O_{12a}(N \rightarrow 12)$	4	**E**	0.24 ± 0.01	4.5 ± 1.8
$O_{12}(11) \rightarrow O_1(12)$; $H{:}O_{12a}(1; 12 \rightarrow 12)$	3	**E**	0.18 ± 0.04	5.7 ± 0.2
		ATc (**2**)		
$H{:}O_{12a}(1 \rightarrow U)$	6	**T**	0.15 ± 0.07	1.7 ± 1.5
$H{:}N_{amine}(3 \rightarrow U)$	5	**T**	0.19 ± 0.00	5.6 ± 0.4
$H{:}O_{12}(11 \rightarrow 1)$	5	**E**, **T**	0.21 ± 0.02	7.8 ± 3.0
$H{:}O_3(A \rightarrow N)$	5	**T**	0.16 ± 0.07	4.2 ± 1.5
$O_{11}(12) \rightarrow O_{12}(11)$	26	**E**, **T**	0.12 ± 0.05	4.5 ± 1.3
$O_{amide}(1) \rightarrow O_1(A)$	11	**E**, **T**	0.06 ± 0.01	1.0 ± 0.5
$O_{amide}(3) \rightarrow O_3(A)$	8	**E**, **T**	0.12 ± 0.06	1.4 ± 1.3
$O_3(A) \rightarrow N_{amine}(3)$	8	**T**	0.18 ± 0.06	1.8 ± 1.5
$O_3(A) \rightarrow N_{amine}(U)$	5	**T**	0.23 ± 0.02	8.1 ± 1.5
$O_{amide}(3) \rightarrow N_{amine}(3)$	3	**T**	0.22 ± 0.00	3.6 ± 0.2
$O_{amide}(3) \rightarrow N_{amine}(U)$	3	**T**	0.19 ± 0.01	9.2 ± 0.3
$N_{amine}(3) \rightarrow O_3(N)$	3	**T**	0.06 ± 0.00	2.3 ± 0.2
$O_3(N) \rightarrow N_{amine}(U)$	3	**T**	0.21 ± 0.01	3.2 ± 0.3
$O_{11}(12) \rightarrow O_{12}(11)$; $H{:}O_{12a}(12 \rightarrow 1; 12)$	5	**E**	0.13 ± 0.01	4.6 ± 0.3
$O_{11}(12) \rightarrow N_{amine}(12a)$; $H{:}O_{12a}(N \rightarrow 12)$	4	**E**	0.19 ± 0.01	8.0 ± 0.3
$O_{11}(12) \rightarrow O_{12}(11)$; $H{:}O_{12a}(1 \rightarrow U)$	3	**T**	0.12 ± 0.10	6.6 ± 1.7
$O_{11}(12) \rightarrow O_{12}(11)$; $H{:}O_3(A \rightarrow N)$	3	**T**	0.21 ± 0.05	9.2 ± 1.7
$O_3(A) \rightarrow N_{amine}(U)$; $H{:}O_{12a}(U \rightarrow 1)$	3	**T**	0.24 ± 0.00	5.4 ± 0.1

[a] Of the 102 shifts found, only those that occurred more than twice and consisted of one hydrogen bond rearrangement, one proton transfer, or one of each are given. The same atom labels are used as in Tables 1 and 2. H:X(Y → Z) describes the hydrogen bond change from XH−Y to XH−Z, whereas W(X) → Y(Z) describes the proton shift from WH−X to YH−Z. The conformation column gives the scaffold conformations for which the change was observed. A and N denote hydrogen bonds to the Me_2N and the amide O, respectively, and U denotes unspecific hydrogen bonding.

both the extended (**1_N1**, **1_N2**, **2_N4**, **2_N5**, **1_N3**, **2_N6**, **2_N7**) and twisted (**1_N9**, **2_N1**, **2_N3**) conformations of the nonionized tautomers and in the extended (**1_Z1**, **1_Z3**, **2_Z2**, **1_Z4**, **2_Z7**, **2_Z9**) zwitterionic conformation.

Charged Structures. The charged structures exhibit variations of the energy differences between the extended and the twisted minima, but the preferred conformation is always conserved. Only slight variations in the internal hydrogen bonds, such as rotation in the $O_{12a}H-O_1;O_{12}$ hydrogen bond toward a pure $O_{12a}H-O_{12}$ bond, exist. The observed, conformation-specific O_{12a} hydrogen bonds are conserved except for some high-energy extended scaffold conformation structures in which an $O_{12a}H-N_{amine}$ hydrogen bond is formed.

TABLE 4: RMSD between the Structures of Tetracycline and 5a,6-Anhydrotetracycline

Tc	ATc	RMSD [Å]
1_N1, **1_N2**	**2_N4**, **2_N5**	0.17
1_N3	**2_N6**, **2_N7**	0.16
1_N9	**2_N1**, **2_N3**	0.24
1_Z1, **1_Z3**	**2_Z2**	0.15
1_Z4	**2_Z7**, **2_Z9**	0.22

For the first deprotonation of Tc, O_3H is preferred in the extended conformation, whereas deprotonation at O_3 or O_{11} is energetically almost equivalent in the twisted scaffold conformations (Table 5). However, the singly deprotonated forms prefer $O_{11}-$ deprotonation for both conformations in ATc. The fully protonated structures of ATc with extended and twisted conformations are energetically identical, but the twisted conformation prefers the O_{amide} over the O_3 protonated tautomer. (Table 5).

Calculated Spin−Spin Coupling Constants. Figure 3 shows the dependence of the calculated $^3J_{HH}(HC_4-HC_{4a})$ coupling constants in vacuo, solvated in water or chloroform, and in systems with different charges on the HC_4-HC_{4a} dihedral angle Θ. Within the limits of accuracy appropriate for this study, the coupling can be approximated as being independent of the solvent and molecular charge. The data can be fitted to the following modified Karplus equation[21] in which the dihedral angle Θ is given in degrees:

$$J_{HH} = 7.5\cos^2(\Theta - 8) + 0.3 \quad (8 < \Theta > 98)$$
$$= 10.8\cos^2(\Theta - 8) + 0.3 \quad (98 < \Theta > 188) \qquad (2)$$

The range separation and agreement between the Tc and ATc $^3J_{HH}(HC_4-HC_{4a})$ spin−spin coupling constants can be used to create characteristic parameters for a "generalized" extended and twisted scaffold conformation (Table 6), enabling us to determine the percentages of extended (P_E) and twisted (P_T) scaffold conformations from the measured NMR data, as described in the Computational Methods section.

Experimental Solvent Conformations of Tetracyclines. The calculated coupling constants for the different conformations of Tc and ATc in solution were compared with the experimental values of the coupling constants of the protons bound to C_4, C_{4a}, C_5, and C_{5a}. The broadening of some signals assigned to the protons on rings A and B suggests that fast tautomeric equilibria exist, as suggested by the DFT calculations. The current data do not, however, allow us to quantify these equilibria.

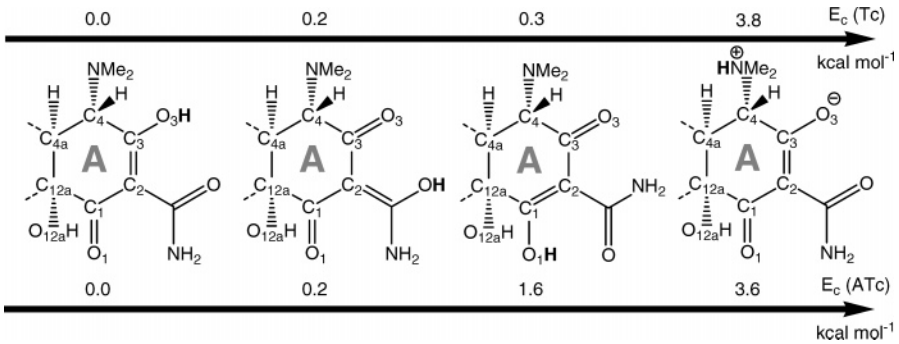

Figure 2. Proton tautomers of ring A and the corresponding relative MP2 energies, E_c, for Tc and ATc. The shifting atom (H) is shown in boldface.

TABLE 5: Conformations, Tautomers, and Energies for the Differently Charged Structures of Tetracycline and 5a,6-Anhydrotetracycline[a]

			protonation state							relative energy			
species	charge	conf	O_{12a}	O_1	O_3	O_{11}	O_{12}	N_{amine}(N)	O_{amide}(A)	0 K	298 K	PCM (H_2O), 298 K	E_c (H_2O)
1_N1_amine	+	**E**	12				11	12a	3	3.7	1.9	0.0	0.0
1_Z1_amine	+	**E**	12				11	12a	3	3.7	1.9	0.2	0.2
1_N9_amine, **1_Z5_amine**	+	**T**	1				11	6	3	0.0	0.0	2.2	1.3
1_N1_O3	−	**E**	N_{amine}				11			2.3	2.6	0.2	0.0
1_N1_O12	−	**E**	N_{amine}		O_{amide}					10.5	9.5	0.0	1.0
1_Z1_O12	−	**E**	12					12a		17.1	17.4	5.5	2.2
1_N9_O12	−	**T**	1		O_{amide}					1.4	1.1	1.5	2.7
1_Z5_O3	−	**T**	1				11			0.5	0.0	0.7	2.8
1_N9_O3	−	**T**	1				11			0.0	0.1	1.7	3.3
1_Z1_O3	−	**E**	1				11			5.0	4.4	2.8	3.6
1_Z5_O12	−	**T**	1					6		22.2	23.8	12.9	9.3
1_N1_O12O3	2−	**E**	N_{amine}							7.4	6.8	0.8	0.0
1_Z5_O12O3	2−	**T**	1							0.0	0.0	0.0	0.7
1_N9_O12O3	2−	**T**	1							0.0	0.0	0.0	0.7
1_Z1_O12O3	2−	**E**	12							1.2	2.2	0.4	1.6
2_N4_amine, 2_Z2_amine	+	**E**	12		O_{amide}	12		12a		0.5	0.2	0.0	0.0
2_Z1_amine	+	**T**	1			12		3	3	0.0	0.6	0.5	0.0
2_N1_amine	+	**T**	1			12		U	3	3.5	3.8	3.8	3.6
2_N1_O11	−	**T**	1		O_{amide}					0.5	0.0	0.0	0.0
2_N1_O3	−	**T**	1			12				0.0	0.8	3.9	1.2
2_N4_O11	−	**E**	N_{amine}		O_{amide}					12.0	11.5	4.3	3.7
2_Z1_O11	−	**T**	1					3		19.1	19.2	9.4	5.0
2_Z1_O3	−	**T**	1			12				6.1	6.8	7.5	5.0
2_Z2_O11	−	**E**	12					12a		19.3	21.1	10.0	5.2
2_Z2_O3	−	**E**	1			12				9.4	9.4	10.7	7.2
2_N4_O3	−	**E**			O_{amide}	12				23.0	22.4	19.6	23.5
2_N1_O11O3	2−	**T**	1							0.0	0.0	0.0	0.0
2_Z1_O11O3	2−	**T**	1							5.0	4.8	3.8	3.5
2_Z2_O11O3	2−	**E**	12							3.9	4.9	4.3	5.1
2_N4_O11O3	2−	**E**			O_{amide}					34.0	32.4	25.1	30.9

[a] Structure designation clarifies the starting structure for the optimization (e.g., **1_N1**) and the location of the protonation/deprotonation. The labeling is analogous to Tables 1 and 2, and protonated/deprotonated atoms are incorporated in the species name. U denotes nonspecific hydrogen bonding.

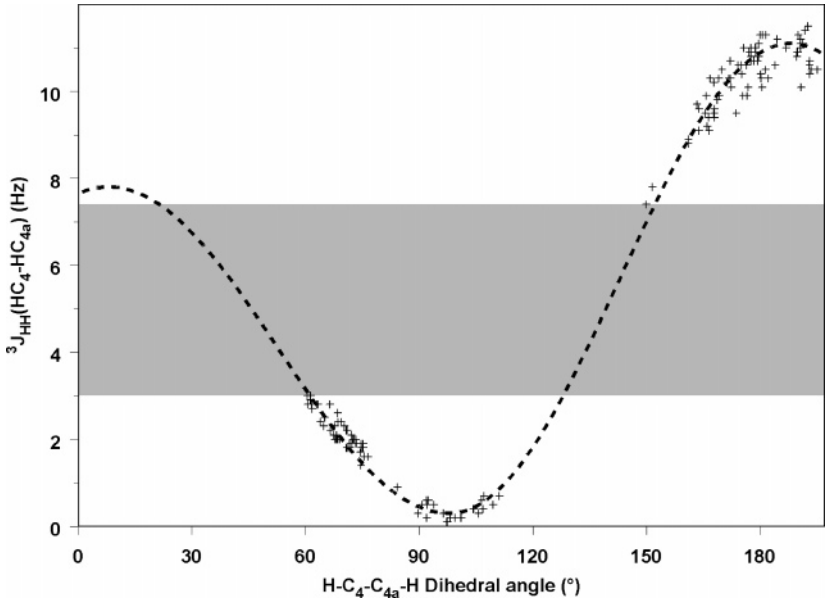

Figure 3. Calculated $^3J_{HH}(HC_4-HC_{4a})$ for extended and twisted Tc and ATc. The dashed curve depicts the modified Karplus equation,[19] as defined in eq 2. The gray area indicates the $^3J_{HH}(HC_4-HC_{4a})$ range that separates the calculated extended and twisted conformations from each other.

The observed coupling constants for Tc are very close to those calculated for the extended conformations. Small coupling constants were found for HC_4 with HC_{4a} and HC_{4a} with HC_5, and a large coupling constant for HC_{4a} with $H'C_5$ was found. These coupling constants remained almost constant in different solvents and at different pH values, suggesting that the

TABLE 6: Range, Mean, and Standard Deviation of the Calculated $^3J_{HH}(HC_4-HC_{4a})$ (Hz) for Different Conformations and Tetracyclines

$^3J_{HH}(HC_4-HC_{4a})$	range	mean ± SD	parameter used
Tc extended	0.1−3.0	1.55 ± 0.98	$cp_E = 1.5$
ATc extended	0.1−3.0	1.52 ± 0.91	
Tc twisted	8.8−11.5	10.42 ± 0.67	$cp_T = 10.3$
ATc twisted	7.4−11.5	10.22 ± 0.87	

conformation does not vary significantly under different conditions (Table 7).

In contrast to Tc, the spectra of ATc indicate conformational flexibility. Whereas, under alkaline conditions (water, pH 10), the coupling constants suggested a conformation more similar to the twisted one, the values observed in nonaqueous solvents and in acidic medium (water, pH 1), particularly those for the couplings of HC_{4a} with $H\alpha C_5$ and $H\beta C_5$, are closer to those for the extended conformation (Table 8).

The percentages of the extended and twisted scaffold conformations calculated from $^3J_{HH}(HC_4-HC_{4a})$ (Table 9) show a clear preference of Tc for the extended conformation. $^3J_{HH}(HC_4-HC_{4a})$ can also be explained without assuming an equilibrium, as the values are located within the range of the calculated spin−spin coupling constants for the extended scaffold conformation. The energy differences between the extended and twisted scaffold conformations resulting from assuming equilibrium are in good agreement with the calculated energy differences. Both the calculations and experiments suggest that the extended conformations are more strongly preferred in neutral water than at alkaline and acidic pHs.

The ATc values measured in water can be explained by assuming a conformational equilibrium between the scaffold conformations. The measured values show a preference for the twisted conformation in alkaline media, an almost equal distribution in neutral water, and a preference for the extended conformation under acidic conditions. The experimental trend toward a larger fraction of twisted conformation in alkaline media is mirrored in the calculations as different scaffold conformations of the fully protonated forms are equal in energy (Table 5) and the deprotonated forms show a preference for the twisted conformation. However, the calculated energy differences of 3.7 and 5.1 kcal mol^{-1} are too large to be compatible with the experimental results. This may be due to incomplete conformational sampling or to deficiencies in the PCM scheme for charged structures. In chloroform, ATc only shows the twisted scaffold conformation, in agreement with the corrected energies, E_c, in chloroform given in Table 10. A comparison with Tables 1 and 2 shows that the preferred conformations are retained, but the detailed minima are different from those found in water and the energetic separation between the twisted and extended conformations increases from 0.2 to 6.2 kcal mol^{-1} for nonionized ATc.

Discussion

Our results demonstrate the power of a combined approach using both measured and calculated NMR coupling constants in order to determine the conformations of tetracyclines in solution, a problem that has proved to be remarkably intractable over the years. The present results allow us to semiquantitatively estimate the proportions of the two major conformations and the free-energy differences. Although there is necessarily a certain amount of noise introduced into our treatment by inaccuracies in the calculated coupling constants and by the simplification of using the single parameters cp_E and cp_T to describe the individual coupling constants of the two conformations, we believe that our results provide relatively accurate assessments of the proportions of the two conformations in solution under the different conditions considered. This allows us to delineate, for the first time, the effects of varying the molecular structure, solvent, or protonation state on the predominant conformation in solution. These data are important because all available X-ray structures of tetracyclines bound to TetR show the inducer in the extended conformation.[24] Thus, Tc adopts the biologically active conformation to a large extent in solution, whereas ATc exists as a mixture of the two major conformers. However, the free-energy penalty in a hypothetical conformational pre-equilibrium is small (0.2 to −0.2 kcal mol^{-1},

TABLE 7: Measured Chemical Shifts and Spin−Spin Coupling Constants for Tetracycline in Different Solvents

		solvent				
proton	NMR parameter	D_2O, pH 1	D_2O, pH 7	D_2O, pH 10	$CDCl_3$	CD_3OD
H-4	δ^a	4.06, br d	3.78, br s	3.24, br d	3.08, br s	3.36, br s
	$J_{HH'}$	1.5	*b*	2.5		
H-4a	δ^a	2.95, ddd	2.75, br d	2.65, ddd	2.64, br d	2.66, ddd
	$J_{HH'}$	13.6, 3.0, 1.5	13.4	13.0, 3.0, 2.5	∼13.0	12.5, 3.0, 3.0
H-5	δ^a	2.28, ddd	2.25, ddd	2.11, ddd	2.00, br d	2.10, ddd
	$J_{HH'}$	13.6, 5.5, 3.0	13.4, 5.4, 3.0	13,4, 5.8, 3.0	∼13.0	13.3, 6.0, 3.0
H-5′	δ^a	1.85, ddd	1.92, ddd	1.78, ddd	1.88, br ddd	1.93, ddd
	$J_{HH'}$	13.6, 13.6, 11.4	13.4, 13.4, 11.4	13.4, 13.0, 11.8	∼13.0, 12.5, 10.0	13.3, 12.5, 10.5
H-5a	δ^a	3.00, dd	3.07, dd	2.89, dd	2.96, dd	2.97, dd
	$J_{HH'}$	11.4, 5.5	11.4, 5.4	11.8, 5.8	10.2, 5.9	10.5, 6.0
$C-CH_3$	δ^a	1.62, s	1.66, s	1.55, s	1.59, s	1.62, s
$N-CH_3$	δ^a	3.05, br s	2.96, s	2.66, s	2.48, br s	2.64, br s
H-7	δ^a	7.20, d	7.24, d	7.06, d	7.09, br d	7.14, d
	$J_{HH'}$	7.8	7.8	7.8	7.8	7.8
H-8	δ^a	7.57, dd	7.61, dd	7.40, dd	7.51, dd	7.50, dd
	$J_{HH'}$	8.2, 7.8	8.2, 7.8	8.2, 7.8	8.4, 7.8	8.4, 7.8
H-9	δ^a	6.98, d	7.03, d	6.87, d	6.95, d	6.91, d
	$J_{HH'}$	8.2	8.2	8.2	8.4	8.4
measured at		300 K	330 K	300 K	270 K	300 K
conformation		**E**	**E**	**E**	**E**	**E**

[a] Chemical shift in ppm and coupling constants in Hz. Multiplicity: s, singlet; d, doublet; dd, doublet of a doublet; br, broad. [b] $J(HC_4-HC_{4a}) < 2$ Hz.

TABLE 8: Measured Chemical Shifts and Spin−Spin Coupling Constants for 5a,6-Anhydrotetracycline in Different Solvents

		solvent				
proton	NMR parameter	D_2O, pH 1	D_2O, pH 7	D_2O, pH 10	$CDCl_3$	CD_3OD
H-4	δ^a	4.12, d	3.91, d	2.90, d	3.30, br d	3.40 br
	$J_{HH'}$	5.0	6.3	6.5	11.0	
H-4a	δ^a	3.41, ddd	3.11, br	2.52, ddd	2.67, br d	2.82, br
	$J_{HH'}$	9.5, 5.0, 5.0		6.5, 5.0, 5.0	11.0	
H-5	δ^a	3.38, dd	3.45, dd	3.17, dd	3.56, br d	3.47, br
	$J_{HH'}$	17.0, 5.0	17.0, 3.2	16.8, 5.0	16.8	16.8
H-5′	δ^a	2.85, dd	3.16, dd	3.13, dd	3.21, br d	3.34, br
	$J_{HH'}$	17.0, 9.5	17.0, 6.8	16.8, 5.0	16.8	
$C-CH_3$	δ^a	2.01, s	2.33, s	2.33, s	2.32, br s	2.48, s
$N-CH_3$	δ^a	3.08, s	2.94, s	2.34, s	2.45, br s	2.55, br s
H-7	δ^a	6.67, d	6.70, d	6.60, d	6.91, d	6.87, dd
	$J_{HH'}$	7.8	7.8	7.8	7.8	7.8, 1.0
H-8	δ^a	7.34, dd	7.54, dd	7.49, dd	7.60, dd	7.59, dd
	$J_{HH'}$	8.4, 7.8	8.3, 7.8	8.4, 7.8	8.4, 7.8	8.4, 7.8
H-9	δ^a	7.00, d	7.32, d	7.24, d	7.42, d	7.50, dd
	$J_{HH'}$	8.4	8.3	8.4	8.4	8.4, 1.0
measured at conformation		300 K **E**	330 K **T**	300 K **T**	230 K **T**	300 K

[a] Chemical shift in ppm and coupling constants in Hz. Multiplicity: s, singlet; d, doublet; dd, doublet of a doublet; br, broad.

TABLE 9: Measured $^3J_{HH}(HC_4-HC_{4a})$, P_E, P_T, and Energy Difference $\Delta E_{E,T}$ between the Twisted and Extended Conformations for Tetracycline and 5a,6-Anhydrotetracycline in Different Solvents

system/solvent	$^3J_{HH}(HC_4-HC_{4a})$	extended (%)	twisted (%)	T (K)	$\Delta E_{E,T}$ (kcal mol^{-1})
Tc/CD_3OD	3	83.0	17.0	300	0.9
Tc/D_2O pH 10	2.5	88.6	11.4	300	1.2
Tc/D_2O pH 7	<2	>94.3	<5.7	330	>1.8
Tc/D_2O pH 1	1.5	100.0	0.0	300	∞
$ATc/CDCl_3$	11	0	100	260	∞
ATc/D_2O pH 10	6.5	43.2	56.8	300	−0.2
ATc/D_2O pH 7	6.3	45.5	54.5	330	−0.1
ATc/D_2O pH 1	5	60.2	39.8	300	0.2

TABLE 10: Corrected MP2 Energies E_c for the Different Conformations of Tetracycline and 5a,6-Anhydrotetracycline in Chloroform

E_c (kcal mol^{-1})	structure	conformation
0.0	**1_N15**	extended
2.6	**1_N9**	twisted
7.4	**1_Z9**	extended
13.5	**1_Z7**	twisted
0.0	**2_N1**	twisted
6.2	**2_N15**	extended
10.3	**2_Z3**	extended
15.4	**2_Z1**	twisted

[a] The structure designations correspond to Tables 1 and 2.

depending on the pH; see Table 9), so that ATc does not suffer a significant conformational disadvantage when binding to TetR.

The measured effect of different solvents on the ATc conformation (Table 9) helps to confirm the effect suggested by calculations[8,9] that the twisted conformation is inherently the more stable conformation in the gas phase but that solvation by polar solvents favors the extended conformation. The twisted conformation predominates in chloroform solution, but the studies in water reveal comparable concentrations of the two conformations at different pHs. The effect of pH is marginal for Tc, for which the extended conformation always predominates, but ATc shows a significant shift from the twisted conformation at a high pH to the extended conformation under acidic conditions. These trends are also suggested by the calculations (Table 5).

The existing experimental evidence is consistent with our data. The trihydrate of the hydrobromide of ATc crystallizes in the extended conformation.[25] Circular dichroism (CD) studies[7] have revealed the influence of pH and especially metal-ion complexation on the conformations of various tetracyclines in solution. The results are also generally compatible with our data, although we do not find the drastic changes in conformation suggested by the CD spectra for tetracycline with changes in pH, but rather a modest shift in the conformation equilibrium from 89:11 extended−twisted at pH 11 to 100:0 at pH 1 (Table 9). It is, however, conceivable that this shift can cause large changes in the CD spectrum.

Conclusions

We have been able to estimate the fractions of the two major conformations of Tc and ATc in several different solvent systems and in water at different pHs. Tc (**1**) prefers the extended conformation under all conditions studied, but the equilibrium is shifted to 100% extended at low pH. The measurements suggest a moderate shift from 91% extended at pH 1 to ≥94% at pH 7 and 100% at pH 1. In contrast, ATc (**2**) prefers the twisted conformation (100%) in chloroform but exhibits more balanced equilibria in water (43:67, 46:64, and 60:40 extended−twisted at pH 1, 7, and 10, respectively).

Comparing calculated and measured NMR coupling constants has proven to be a valuable technique for investigating Tc conformational equilibria. We are now extending our studies to be able to estimate tautomeric equilibria by the comparison of calculated and experimental NMR data, although this represents a far more formidable task than estimating the conformational equilibria.

Acknowledgment. This work was supported by the Deutsche Forschungsgemeinschaft as part of SFB 473 (Mechanisms of

Transcriptional Regulation) and GraKo 805 (Protein−Protein Interactions in Signal Transduction).

Supporting Information Available: A ZIP archive containing a Microsoft Excel file with the calculated energies for the species reported in this paper (Tables 1, 2, 5, and 10; unabridged) as well as all optimized geometries. This material is available free of charge via the Internet at http://pubs.acs.org.

References and Notes

(1) Barza, M.; Schiefe, R. T. *Am. J. Hosp. Pharm.* **1977**, *34*, 49−57.

(2) (a) Saenger, W.; Orth, P.; Kisker, C.; Hillen, W.; Hinrichs, W. *Angew. Chem., Int. Ed.* **2000**, *39*, 2042−2052. (b) Lanig, H.; Othersen, O. G.; Beierlein, F. R.; Seidel, U.; Clark, T. *J. Mol. Biol.* **2006**, *359*, 1125−1136.

(3) Scholz, O.; Schubert, P.; Kintrup, M.; Hillen, W. *Biochemistry* **2000**, *39*, 10914−10920.

(4) Lanig, H.; Othersen, O. G.; Seidel, U.; Beierlein, F. R.; Exner, T.; Clark, T. *J. Med. Chem.* **2006**, *49*, 3444−3447.

(5) Restivo, R.; Palenik, G. J. *Biochem. Biophys. Res. Commun.* **1969**, *36* (4), 621−624.

(6) (a) Mazzola, E. P.; Melin, J. A.; Wayland, L. G. *J. Pharm. Sci.* **1980**, *69* (2), 229−230. (b) Celotti, M.; Fazakerley, G. V. *J. Chem. Soc., Perkin Trans. 2* **1977**, 1319−1322. (c) Asleson, G. L.; Frank, C. W. *J. Am. Chem. Soc.* **1976**, *98* (16), 4745−4749. Asleson, G. L.; Stoel, L. J.; Newman, E. C.; Frank, C. W. *J. Pharm. Sci.* **1974**, *63* (7), 1144−1146.

(7) (a) Mitscher, L. A.; Bonacci, A. C.; Sokoloski, T. D. *Tetrahedron Lett.* **1968**, *10*, 5361−5364. (b) Stezowski, J. J. *Kem. Kozl.* **1983**, *60* (1−2), 2−9. (c) Prewo, R.; Stezowski, J. J. *J. Am. Chem. Soc.* **1980**, *102* (23), 7015−7020. (d) Hughes, L. J.; Stezowski, J. J.; Hughes, R. E. *J. Am. Chem. Soc.* **1979**, *101* (26), 7655−7656. (e) Grosheva, V. I. *Antibiot. Khimioter.* **1992**, *37*, 11−14.

(8) Othersen, O. G.; Beierlein, F.; Lanig, H.; Clark, T. *J. Phys. Chem. B* **2003**, *107*, 13743−13749.

(9) Meindl, K.; Clark, T. *J. Phys. Chem. B* **2005**, *109*, 4279−4284.

(10) (a) Leypold, C. F.; Reiher, M.; Brehm, G.; Schmitt, M. O.; Schneider, S.; Matousek, P.; Towrie, M. *Phys. Chem. Chem. Phys.* **2003**, *5* (6), 1149−1157. (b) Dos Santos, H. F.; Nascimento, C. S.; Belletato, P.; De Almeida, W. B. *THEOCHEM* **2003**, *626*, 305−319.

(11) Miertus, S.; Scrocco, E.; Tomasi, J. *Chem. Phys.* **1981**, *55*, 117−129.

(12) Frisch, M. J.; et al. *Gaussian 98*; Gaussian, Inc.: Pittsburgh, PA, 1998.

(13) Frisch, M. J.; et al. *Gaussian 03*; Gaussian, Inc.: Pittsburgh, PA, 2003.

(14) (a) Becke, A. D. *J. Chem. Phys.* **1993**, *98*, 1372. (b) Becke, A. D. *J. Chem. Phys.* **1993**, *98*, 5648. (c) Stephens, P. J.; Devlin, F. J.; Chabalowski, C. F.; Frisch, M. J. *J. Phys. Chem.* **1994**, *98*, 11623. (d) Becke, A. D. *J. Chem. Phys.* **1993**, *98*, 5648. (e) Becke, A. D. In *The Challenge of d- and f-Electrons: Theory and Computation*; Salahub, D. R., Zerner, M. C., Eds.; American Chemical Society: Washington, DC, 1989; Chapter 12, pp 165−179. (f) Vosko, S. H.; Wilk, L.; Nusait, M. *Can. J. Phys.* **1980**, *58*, 1200−1211.

(15) Lee, C.; Yang, W.; Parr, R. G. *Phys. Rev. B* **1988**, *37*, 785−789.

(16) (a) Ditchfield, R.; Hehre, W. J.; Pople, J. A. *J. Chem. Phys.* **1971**, *54*, 724−728. (b) Hehre, W. J.; Ditchfield, R.; Pople, J. A. *J. Chem. Phys.* **1972**, *56*, 2257−2261. (c) Hariharan, P. C.; Pople, J. A. *Mol. Phys.* **1974**, *27*, 209−214. (d) Gordon, M. S. *Chem. Phys. Lett.* **1980**, *76*, 163−168. (e) Hariharan, P. C.; Pople, J. A. *Theor. Chim. Acta* **1973**, *28*, 213−222.

(17) Barone, V.; Cossi, M.; Tomasi, J. *J. Chem. Phys.* **1997**, *107*, 3210−3221.

(18) (a) Frisch, M. J.; Head-Gordon, M.; Pople, J. A. *Chem. Phys. Lett.* **1990**, *166*, 275−280. (b) Frisch, M. J.; Head-Gordon, M.; Pople, J. A. *Chem. Phys. Lett.* **1990**, *166*, 281−289. (c) Pople, J. A.; Krishnan, R.; Schlegel, H. B.; Binkley, J. S. *Int. J. Quantum Chem., Quantum Chem. Symp.* **1975**, *13*, 325; **1979**, *17*, 225−241. (d) Handy, N. C.; Schaefer, H. F., III. *J. Chem. Phys.* **1984**, *81*, 5031−5033.

(19) Heisterberg, D.; Labanowski, J. Quatfit. http://ccl.net/cca/software/SOURCES/C/quaternion-mol-fit/index.shtml.

(20) (a) Wolinski, K.; Hinton, J. F.; Pulay, P. *J. Am. Chem. Soc.* **1990**, *112*, 8251−8260. (b) Dodds, J. L.; McWeeny, R.; Sadlej, A. J. *Mol. Phys.* **1980**, *41*, 1419. (c) McWeeny, R. *Chem. Phys. Lett.* **1971**, *9* (4), 341−2. (d) Ditchfield, R. *Mol. Phys.* **1974**, *27*, 789−807.

(21) (a) Karplus, M. *J. Chem. Phys.* **1959**, 30, 11−15. (b) Karplus, M. *J. Am. Chem. Soc.* **1963**, *85*, 2870−2871.

(22) Günther, H. *NMR−Spektroskopie 3. Auflage*; Thieme Verlag: Stuttgart, Germany, 1992.

(23) Bax, A. *J. Magn. Reson.* **1985**, *65*, 142−145.

(24) (a) Hinrichs, W.; Kisker, C.; Duvel, M.; Muller, A.; Tovar, K.; Hillen, W.; Saenger, W. *Science (Washington, DC, U.S.)* **1994**, *264* (5157), 418−420. (b) Kisker, C.; Hinrichs, W.; Tovar, K.; Hillen, W.; Saenger, W. *J. Mol. Biol.* **1995**, *247*, 260−280. (c) Orth, P.; Saenger, W.; Hinrichs, W. *Biochemistry* **1999**, *38* (1), 191−198. (d) Orth, P.; Schnappinger, D.; Sum, P. E.; Ellestad, G. A.; Hillen, W.; Saenger, W.; Hinrichs, W. *J. Mol. Biol.* **1999**, *285*, 455−461. (e) Orth, P.; Schnappinger, D.; Hillen, W.; Saenger, W.; Hinrichs, W. *Nat. Struct. Biol.* **2000**, *7*, 215−219.

(25) Palenik, G. J.; Mathew, M.; Restivo, R. *J. Am. Chem. Soc.* **1978**, *100*, 4458−4464.